

- 13 D. J. Chadi and N. Troullier, *Physica B* **185**, 128 (1993).
- 14 B.-H. Cheong, C. H. Park, and K. J. Chang, to be published.
- 15 A. Garcia and J. E. Northrup, *Phys. Rev. Lett.* **74**, 1131 (1995).
- 16 G. D. Watkins, in *Defect Control in Semiconductors*, edited by K. Sumino (Elsevier Science Publishers B. V., Amsterdam, 1990), p. 933.
- 17 G.-X. Qian, R. M. Martin, and D. J. Chadi, *Phys. Rev. B* **38**, 7649 (1988); N. Chetty and R. M. Martin, *ibid.* **45** 6089 (1992).
- 18 P. Hohenberg and W. Kohn, *Phys. Rev.* **136**, B864 (1964); W. Kohn and L. J. Sham, *ibid.* **140**, A1133 (1965).
- 19 D. R. Hamann, M. Schlüter, and C. Chiang, *Phys. Rev. Lett.* **43**, 1494 (1979).
- 20 N. Troullier and J. L. Martins, *Phys. Rev. B* **43**, 1993 (1991).
- 21 D. B. Laks, C. G. Van de Walle, G. F. Neumark, P. E. Blochl, and S. T. Pantelides, *Phys. Rev. B* **45**, 10965 (1992).
- 22 R. Stumpf and M. Scheffler, *Computer Phys. Commun.* **79**, 447 (1994).
- 23 J. Neugebauer, to be published.
- 24 J. Neugebauer and C. G. Van de Walle, in *Diamond, SiC and Nitride Wide Bandgap Semiconductors*, edited by C. H. Carter Jr., G. Gildenblat, S. Nakamura, and R. J. Neumark, Materials Research Society Symposium Proceedings, Vol. 339 (Materials Research Society, Pittsburgh, Pennsylvania), p. 687.
- 25 D. B. Laks, C. G. Van de Walle, G. F. Neumark, and S. T. Pantelides, *Appl. Phys. Lett.* **63**, 1375 (1993).
- 26 C. G. Van de Walle and D. B. Laks, *Solid State Communications* **93**, 447 (1995).
- 27 We estimated that relaxation energies would not exceed 1 eV.
- 28 K. Ando, Y. Kawaguchi, T. Ohno, A. Ohki, and S. Zembutsu, *Appl. Phys. Lett.* **63**, 191 (1993).
- 29 I. S. Hauksson, J. Simpson, S. Y. Wang, K. A. Prior, and B. C. Cavenett, *Appl. Phys. Lett.* **61**, 2208 (1992).
- 30 B. N. Murdin, B. C. Cavenett, C. R. Pidgeon, J. Simpson, I. S. Hauksson, and K. A. Prior, *Appl. Phys. Lett.* **63**, 2411 (1993).
- 31 T. Marshall, *Physica B* **185**, 433 (1993).
- 32 Y. Nishikawa, M. Ishikawa, S. Saito, and G. Hatakoshi, *Jpn. J. Appl. Phys.* **33**, L361 (1994).
- 33 S. Ito, M. Ikeda, and K. Akimoto, *Jpn. J. Appl. Phys.* **31**, L1316 (1992).
- 34 K. Shahzad, B. A. Khan, D. J. Olego, and D. A. Carnack, *Phys. Rev. B* **42**, 11 240 (1990).
- 35 P. M. Mensz, *J. Cryst. Growth*, **138**, 697 (1994).
- 36 Y. Fan, J. Han, L. He, R. L. Gunshor, M. S. Brandt, J. Walker, N. M. Johnson, and A. V. Nurmikko, *Appl. Phys. Lett.* **65**, 1001 (1994).
- 37 K. W. Kwak, D. Vanderbilt, and R. D. King-Smith, submitted to *Phys. Rev. B*.
- 38 J. Qiu, J. M. DePuydt, H. Cheng, and M. A. Haase, *Appl. Phys. Lett.* **59**, 2992 (1991).
- 39 L. H. Kuo, L. Salamanca-Riba, J. M. DePuydt, H. Cheng, and J. Qiu, *Appl. Phys. Lett.* **63**, 3197 (1993).
- 40 J. M. DePuydt, private communication.
- 41 J. Neugebauer and C. G. Van de Walle, to be published.
- 42 J. Neugebauer and C. G. Van de Walle, in *Proceedings of the 22th International Conference on the Physics of Semiconductors*, Vancouver, 1994 (World Scientific Publishing Co Pte Ltd., Singapore), p. 2327.

THE ROLE OF IMPURITIES IN HYDRIDE VAPOR PHASE EPITAXIALLY GROWN GALLIUM NITRIDE

R. J. Molnar, K. B. Nichols, P. Maki, E. R. Brown and I. Melngailis
Massachusetts Institute of Technology, Lincoln Laboratory, Lexington, MA 02175-9108

ABSTRACT

Gallium nitride (GaN) films grown by hydride vapor phase epitaxy on a variety of substrates have been investigated to study what role silicon and oxygen impurities play in determining the residual donor levels found in these films. Secondary ion mass spectroscopy analysis has been performed on these films and impurity levels have been normalized to ion implanted calibration standards. While oxygen appears to be a predominate impurity in all of the films, in many of them the sum of silicon and oxygen levels is insufficient to account for the donor concentration determined by Hall measurements. This suggests that either another impurity or a native defect is at least partly responsible for the autodoping of GaN. Additionally, the variation of impurity and carrier concentration with surface orientation and/or nucleation density suggests either a crystallographic or defect-related incorporation mechanism.

INTRODUCTION

Recently, hydride vapor phase epitaxy (HVPE) of gallium nitride (GaN) has regained attention, primarily as a quasi-bulk technique to grow thick, free-standing films for use as substrates in the growth of device structures by other techniques, such as metalorganic vapor phase epitaxy (MOVPE) or molecular beam epitaxy (MBE)¹. While the literature is rich with studies of this growth technique, there has been wide speculation as to the origin of the residual donors in these films. Maruska and Tietjen speculated that these residual donors might be nitrogen vacancy native defects². While it has been subsequently shown both experimentally³ and theoretically⁴ that nitrogen vacancies are not likely, defect aggregates, possibly involving such a vacancy, cannot be ruled out.

Of course, a very important question is whether the residual donors in GaN (as well as InGaN) films can be completely accounted for by impurities. For example, it has been observed in the HVPE growth of Al-bearing films that strong exchange reactions between AlCl compounds and quartz reactor walls result in extremely high Si and O concentrations in films⁵. It is possible that, at the elevated temperatures (~1100°C) used in the growth of GaN, similar reactions could take place with GaCl compounds. Illegans and Montgomery⁶ have reported that impurity levels in their films were insufficient to completely account for the residual donors in their HVPE-grown films. However, their analytical methods, namely, spark source spectroscopy or uncalibrated secondary ion mass spectroscopy (SIMS), were not effective in accurately determining the impurities in these films, particularly for oxygen, which is known to act as a donor in GaN⁷. In this paper, therefore, we have investigated the residual donors in GaN films by Hall measurements as well as the concentration of suspected donors, i.e., silicon and oxygen, by calibrated SIMS analysis. Our results show that while oxygen is a predominate impurity, the sum of silicon and oxygen levels in many of the films is insufficient to account for the donor concentration observed in these films. In fact, the rather large ionization energy of oxygen donors (~78 meV)⁸ as well as compensation expected in such films strengthen the argument that the electron transport properties of GaN are at least partly determined by an as yet unidentified donor, either an impurity or native defect. Our results are consistent with the literature in suggesting that the incorporation of this defect as well as impurities such as oxygen and silicon is intimately related to the growth conditions, particularly during heteronucleation.

EXPERIMENTAL

$\text{HCl} + \text{H}_2$ $\text{NH}_3 + \text{N}_2 + \text{Dopants}$

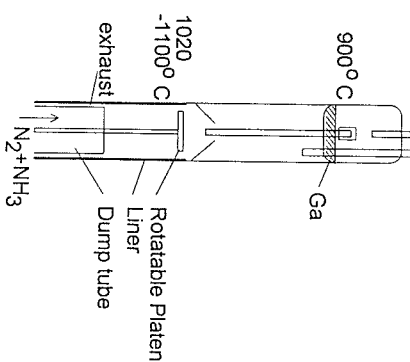


Figure 1-Schematic of HVPE reactor.

2000 sccm N_2 (main carrier). Under such conditions, growth rates of $\sim 30\text{-}50\text{ }\mu\text{m/h}$ are typical depending on substrate position.

The surface morphology was investigated by both optical and electron microscopy. The films grown directly on (0001) Al_2O_3 exhibited a faceted hillock structure, as shown in Figure 2(a-d). The surfaces of these hillocks were defined predominantly by $\{110\}$ planes which gave way to (0001)-truncated surfaces with increasing growth temperature or decreasing growth rate, as has been observed in GaN films grown by MOVPE⁸. Additionally, by utilizing GaCl pretreatment methods described by Naniwae et al.,⁹ we have been able to obtain smooth, featureless surfaces, as shown in Figure 3. These optically transparent films were determined to be single crystals by X-ray diffraction (XRD) with a high degree of internal cracking due to thermal stress at the GaN/ Al_2O_3 interface.

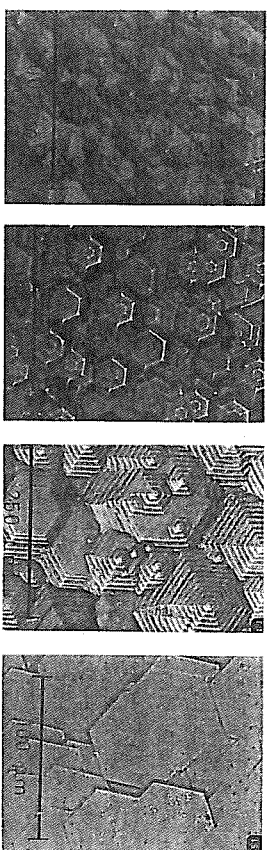


Figure 2 - Various surface morphologies obtained on (0001) Al_2O_3 .

The films in this study were grown by a

modified version of the chloride-transport HVPE process described by Maruska and Tiejen.² In this process the Ga precursor is synthesized upstream in the reactor via a reaction of HCl gas (in an H_2 diluent) with Ga metal (at 900°C) to form GaCl. This precursor is then transported to the substrate area where it is mixed with NH_3 (in an N_2 carrier) to form GaN (at $\sim 1100^\circ\text{C}$). Our reactor differs from Maruska's in that the growth tube is arranged vertically to allow rotation of the substrate during growth to improve uniformity. Additionally, we have provisions to lower the substrate platen isothermally into a dump tube in which we counterflow NH_3 in a N_2 carrier (see Figure 1). This allows us to abruptly interrupt the growth and either change and equilibrate the flow of gas species in the main tube or slowly cool the substrate by further lowering the platen at the end of the growth.

Typical flow rates in our system are 5 sccm HCl, 450 sccm NH_3 , 100 sccm H_2 (HCl diluent), and

process the Ga precursor is synthesized upstream in

the reactor via a reaction of HCl gas (in an H_2 diluent) with Ga metal (at 900°C) to form GaCl.

This precursor is then transported to the substrate area where it is mixed with NH_3 (in an N_2 carrier) to form GaN (at $\sim 1100^\circ\text{C}$). Our reactor differs from Maruska's in that the growth tube is arranged vertically to allow rotation of the substrate during growth to improve uniformity. Additionally, we have provisions to lower the substrate platen isothermally into a dump tube in which we counterflow NH_3 in a N_2 carrier (see Figure 1). This allows us to abruptly interrupt the growth and either change and equilibrate the flow of gas species in the main tube or slowly cool the substrate by further lowering the platen at the end of the growth.

Typical flow rates in our system are 5 sccm HCl, 450 sccm NH_3 , 100 sccm H_2 (HCl diluent), and

process the Ga precursor is synthesized upstream in the reactor via a reaction of HCl gas (in an H_2 diluent) with Ga metal (at 900°C) to form GaCl.

This precursor is then transported to the substrate area where it is mixed with NH_3 (in an N_2 carrier) to form GaN (at $\sim 1100^\circ\text{C}$). Our reactor differs from Maruska's in that the growth tube is arranged vertically to allow rotation of the substrate during growth to improve uniformity. Additionally, we have provisions to lower the substrate platen isothermally into a dump tube in which we counterflow NH_3 in a N_2 carrier (see Figure 1). This allows us to abruptly interrupt the growth and either change and equilibrate the flow of gas species in the main tube or slowly cool the substrate by further lowering the platen at the end of the growth.

Typical flow rates in our system are 5 sccm HCl, 450 sccm NH_3 , 100 sccm H_2 (HCl diluent), and

process the Ga precursor is synthesized upstream in the reactor via a reaction of HCl gas (in an H_2 diluent) with Ga metal (at 900°C) to form GaCl.

This precursor is then transported to the substrate area where it is mixed with NH_3 (in an N_2 carrier) to form GaN (at $\sim 1100^\circ\text{C}$). Our reactor differs from Maruska's in that the growth tube is arranged vertically to allow rotation of the substrate during growth to improve uniformity. Additionally, we have provisions to lower the substrate platen isothermally into a dump tube in which we counterflow NH_3 in a N_2 carrier (see Figure 1). This allows us to abruptly interrupt the growth and either change and equilibrate the flow of gas species in the main tube or slowly cool the substrate by further lowering the platen at the end of the growth.

Typical flow rates in our system are 5 sccm HCl, 450 sccm NH_3 , 100 sccm H_2 (HCl diluent), and

process the Ga precursor is synthesized upstream in the reactor via a reaction of HCl gas (in an H_2 diluent) with Ga metal (at 900°C) to form GaCl.

This precursor is then transported to the substrate area where it is mixed with NH_3 (in an N_2 carrier) to form GaN (at $\sim 1100^\circ\text{C}$). Our reactor differs from Maruska's in that the growth tube is arranged vertically to allow rotation of the substrate during growth to improve uniformity. Additionally, we have provisions to lower the substrate platen isothermally into a dump tube in which we counterflow NH_3 in a N_2 carrier (see Figure 1). This allows us to abruptly interrupt the growth and either change and equilibrate the flow of gas species in the main tube or slowly cool the substrate by further lowering the platen at the end of the growth.

Typical flow rates in our system are 5 sccm HCl, 450 sccm NH_3 , 100 sccm H_2 (HCl diluent), and

process the Ga precursor is synthesized upstream in the reactor via a reaction of HCl gas (in an H_2 diluent) with Ga metal (at 900°C) to form GaCl.

This precursor is then transported to the substrate area where it is mixed with NH_3 (in an N_2 carrier) to form GaN (at $\sim 1100^\circ\text{C}$). Our reactor differs from Maruska's in that the growth tube is arranged vertically to allow rotation of the substrate during growth to improve uniformity. Additionally, we have provisions to lower the substrate platen isothermally into a dump tube in which we counterflow NH_3 in a N_2 carrier (see Figure 1). This allows us to abruptly interrupt the growth and either change and equilibrate the flow of gas species in the main tube or slowly cool the substrate by further lowering the platen at the end of the growth.

Typical flow rates in our system are 5 sccm HCl, 450 sccm NH_3 , 100 sccm H_2 (HCl diluent), and

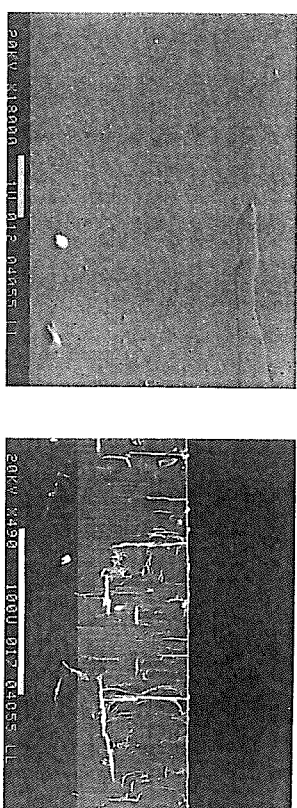


Figure 3 - Scanning electron micrographs of surface morphology and cross section of GaN film deposited using GaCl pretreatment.

In addition to the growth directly on (0001) Al_2O_3 , we have investigated the use of sputtered ZnO buffer layers as reported by Detchprohm et al.¹ The films were deposited in an RF sputtering system with a 5 in. diameter cathode, a 1:1 mixture of O_2 and Ar at 20 mT and RF power levels of 200 W. Reflection high energy electron diffraction patterns obtained from such buffers show a high degree of in-plane orientation with noticeable twinning, as shown in Figure 4. GaN films deposited on these buffers exhibit uniform film growth with large, low-angle hillocks indicative of a high lateral growth rate, as shown in Figure 5(a). Additionally, a small number of these hillocks ($<5\%$) show spiral growth emanating from screw dislocations, as shown in Figure 5(b). To our knowledge, this is the first report of such defects observed in GaN. The dimensions of these features again indicate the high lateral growth rate.

We also investigated several other orientations of sapphire, namely the $(1\bar{1}00)$ and $(11\bar{2}0)$ planes, as well as (0001) off-axis Si-faced SiC substrates. For GaN films deposited on the $(1\bar{1}00)$ plane of Al_2O_3 , XRD indicate them to be monocrystalline and $(1\bar{1}03)$ oriented, similar to that reported by Hwang et al.¹⁰ The GaN films grown on $(11\bar{2}0)$ Al_2O_3 surfaces show (0001) orientation, as is commonly observed. The surface morphologies of these films are represented in Figure 6. It is interesting to note that while (0001) oriented GaN grown on (0001) Al_2O_3 , ZnO and SiC or $(11\bar{2}0)$ Al_2O_3 showed thermally induced cracking originating from the substrate/GaN interface, the GaN film grown on the $(1\bar{1}00)$ Al_2O_3 substrate did not. This may account for the somewhat higher mobility obtained for this orientation, as listed in Table I.

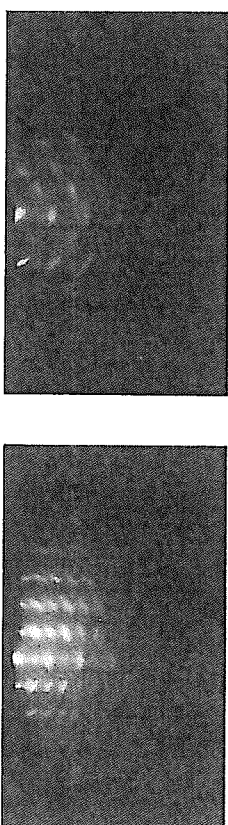


Figure 4 - Reflection high energy electron diffraction pattern obtained from ZnO buffer.

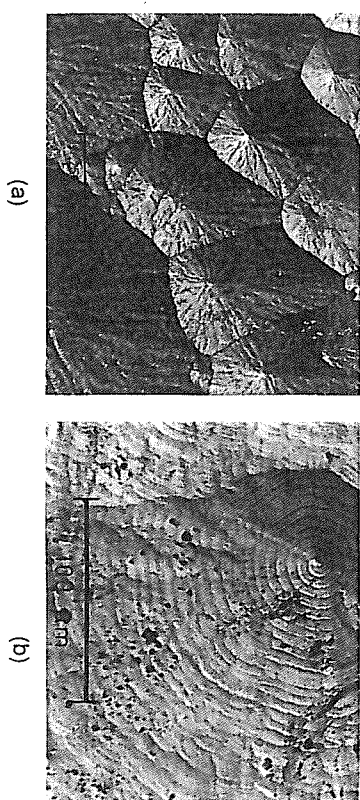


Figure 5 - Surface morphology of GaN films deposited on ZnO buffer.

The van der Pauw geometry was used to investigate the transport properties of the films. Rectangular pieces, ~5 mm on edge, were contacted with In solder and measured at room temperature in a magnetic field of 0.5 T and with a test current of 10 mA. For the sample shown in Figure 3, the severity of the thermal cracking led to excessive asymmetry in the measurements prohibiting accurate determination of the transport properties. However, the ability to readily form rectifying tungsten contacts with high breakdown voltage (~200 V) on this material suggests that the films are nondegenerate. Impurities levels in these films were determined by SIMS analysis using a Cs sputter beam and comparing signal levels with those obtained from ion-implanted GaN calibration standards¹¹. It is reasonable to expect that impurity concentrations determined by such normalization are accurate to within a factor of two. Table I shows the transport properties and impurity concentrations for Si, O and C as well as several other common impurities in the HVPE GaN films. A \leq sign indicates that impurity levels were at or below the detection limit indicated. For comparison, we have also indicated the results of SIMS analysis on an electron cyclotron resonance (ECR) plasma assisted MBE grown GaN film from our group. This sample was grown directly on (0001) Al₂O₃ in a similar fashion to Mohar et al.¹² except for the liner of the plasma source in this case being fabricated from pyrolytic boron nitride.

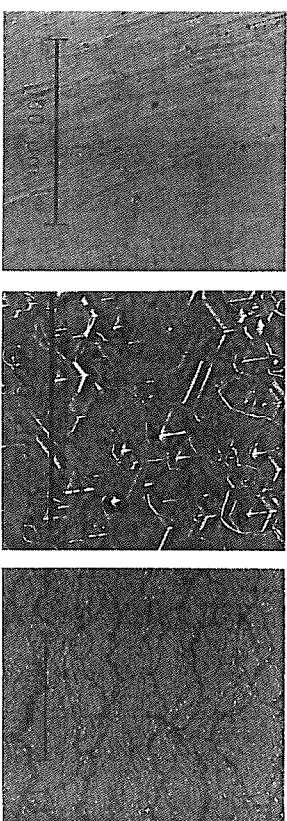


Figure 6 - Typical surface morphology for GaN films deposited on (a) (1100) Al₂O₃, (b) (1120) Al₂O₃ and (c) (0001) SiC.

Table I - Material parameters of GaN films obtained from Hall and SIMS measurements.

| Substrate | Growth Method | μ (cm ² /V.s) | n (cm ⁻³) | SIMS Impurity Concentration (cm ⁻³) | | | | | |
|--------------------------------|---------------|------------------------------|-------------------------|---|--------------------|-------------------------|--------------------|-------------------------|-------------------------|
| | | | | Si | O | C | H | Cl | F |
| (0001) | HVPE | 124 | 1.0×10^{19} | 3×10^{17} | 3×10^{18} | 2×10^{16} | 7×10^{17} | 2×10^{16} | $\leq 1 \times 10^{15}$ |
| Al ₂ O ₃ | | | | | | | | | |
| (0001) | HVPE | 57 | 3.7×10^{18} | 4×10^{15} | 5×10^{17} | $\leq 5 \times 10^{15}$ | 8×10^{16} | 2×10^{16} | $\leq 4 \times 10^{14}$ |
| Al ₂ O ₃ | | | | | | | | | |
| (1120) | HVPE | 44 | 4.6×10^{17} | $\leq 3 \times 10^{15}$ | 5×10^{17} | $\leq 5 \times 10^{15}$ | 4×10^{18} | 2×10^{17} | $\leq 4 \times 10^{14}$ |
| Al ₂ O ₃ | | | | | | | | | |
| (1100) | HVPE | 156 | 1.5×10^{18} | 8×10^{15} | 2×10^{18} | $\leq 2 \times 10^{16}$ | 2×10^{17} | $\leq 7 \times 10^{15}$ | $\leq 1 \times 10^{15}$ |
| Al ₂ O ₃ | | | | | | | | | |
| (0001) | HVPE | 93 | 1.7×10^{17} | $\leq 4 \times 10^{15}$ | 2×10^{18} | $\leq 5 \times 10^{15}$ | 3×10^{17} | 1×10^{17} | $\leq 4 \times 10^{14}$ |
| ZnO | | | | | | | | | |
| (0001) | HVPE | 125 | 1.6×10^{19} | 4×10^{16} | 1×10^{18} | 2×10^{16} | 2×10^{17} | 1×10^{16} | $\leq 6 \times 10^{14}$ |
| SiC | | | | | | | | | |
| (0001) | ECR-MBE | 270 | 2.5×10^{17} | $\leq 2 \times 10^{15}$ | 2×10^{18} | 4×10^{16} | 4×10^{19} | 4×10^{15} | 7×10^{15} |

DISCUSSION

It is clear from the SIMS data that the HVPE films typically show low levels of carbon impurities, in many cases below the detection limit. This is likely the result of the high purity of the source materials, the extremely high growth rate and the inherent lack of hydrocarbon radicals in the Ga precursor, in contrast with MOVPE. This may also explain why HVPE GaN typically shows lower carrier compensation than material grown by other methods. The predominant impurity appears to be oxygen. While the source of this impurity is not yet known, reduction of the quartz cannot be ruled out. In films where dense, uniform nucleation is achieved, as is the case for the film grown on sputtered ZnO, the incorporation of impurities as well as residual donors is reduced. In fact, the film grown on the ZnO buffer shows oxygen and donor levels about a factor of ten lower than the other samples investigated. This is surprising in light of the inherent thermal instability of the ZnO buffer.

For convenience, the data of Table I is plotted in Figure 7 as the sum of suspected donor impurities (Si and O) vs room temperature carrier concentration. It is clear from the data that the residual donor levels, in at least some of these films, cannot be accounted for by the sum of the silicon and oxygen levels, even if one were to assume that these defects were completely ionized at room temperature. The data does, however, suggest that the incorporation of these impurities in the films is correlated with the growth conditions in similar ways as the undetermined donor. In particular, the nucleation and surface crystallography appear to play predominant roles in impurity incorporation, either through a crystallographic or defect-mediated process. Finally, it is important to note that, for the sample grown by ECR-MBE, the reduction in Si and O over those reported previously¹³ reinforces the notion that the quartz liner used in the previous study was a source of impurities in the GaN films.

CONCLUSIONS

GaN films have been grown by HVPE. The role that impurities play in determining the electronic properties of these films has been investigated. In particular, the levels of Si and O in some of the films was found to be insufficient to account for the observed donor concentrations.

HIGH RESISTIVITY IN AlN BY NITROGEN OR OXYGEN IMPLANTATION

J. C. ZOLPER,^a S. J. PEARTON,^b C. R. ABERNATHY,^b and C. B. VARTULI,^b
^aSandia National Laboratories, Albuquerque, NM 87185-0603,
^bUniversity of Florida, Department of Materials Science and Engineering,
 Gainesville, FL 32611

ABSTRACT

We report on the isolation properties of In_{0.75}Al_{0.25}N implanted with either N or O for several doses and post-implant anneal temperatures. Sheet resistance versus anneal temperature data are reported for the various implants with a maximum sheet resistance of $\sim 1 \times 10^9 \Omega/\square$ achieved for a high dose N-implant annealed at 600 °C and $\sim 5 \times 10^8 \Omega/\square$ achieved for a high dose O-implant annealed at 600 °C. These sheet resistances correspond to a greater than three order of magnitude increase over the as-grown values. The compensating defect level for the highest resistance N-implanted sample has an estimate ionization level 580 meV below the conduction band edge. Implant isolation of InAlN is also compared to oxygen implant isolation of InGa_{1-x}N -- where only a 50 to 100 fold increase in sheet resistance is observed -- to study the effect of Al in the isolation scheme.

INTRODUCTION

The III-V nitride-containing semiconductors InN, GaN, and AlN and their ternary alloys are attracting renewed interest for application to visible light emitters^{1,2} and as the basis for high temperature electronics.³⁻⁵ Their attractive material properties include bandgaps ranging from 1.9 eV (InN) to 6.2 eV (AlN), an energy gap ($E_g(\text{GaN}) = 3.39 \text{ eV}$) matched to the short wavelength region of the visible spectrum, high breakdown fields, and relatively high carrier mobilities.⁶ For heterostructure field effect transistors (HFETs) and heterostructure LEDs and lasers, Al-containing ternaries should play a role as a barrier or modulation doping layer. In addition, for HFET structures, thermally stable implant isolation of the Al-containing layer will be desirable.

There have been limited reports of the implantation properties of the III-V nitrides or, in particular, the isolation properties of In-containing III-V nitrides. Early work by Pankove⁷ focused on the optical properties of GaN implanted with an array of elements while Khan investigated the implantation of Be or N in GaN⁸ and AlGaN⁹ to improve Schottky barrier characteristics. For In-containing material the first report of their isolation properties was for F-implant In_{0.37}Ga_{0.63}N and In_{0.75}Al_{0.25}N for one dose.¹⁰ The F-implanted InAlN showed roughly a factor of 10 increase in sheet resistance to $\sim 5 \times 10^6 \Omega/\square$ after implantation and annealing at 500 °C while the InGaN displayed a similar trend but with a slightly lower peak sheet resistance. More recently, the isolation properties of a range of In-fractions of InGaN has been reported for both F, N, and O implantation at several doses.^{11,12} In addition, implant isolation of p- and n-type GaN by N-implantation has also recently been demonstrated.¹³

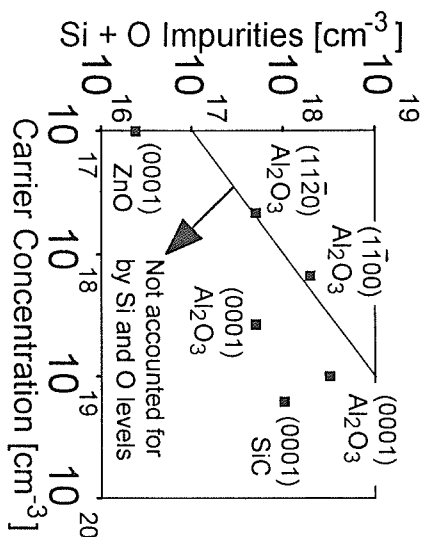


Figure 7 - SIMS O + Si levels vs carrier concentration for HVPE films investigated.
 This suggests that either a native defect or undetermined impurity is at least partially responsible for the observed autodoping behavior in GaN.

ACKNOWLEDGEMENTS

The authors gratefully acknowledge the technical assistance of D. Hovey, R. Murphy, G. Iseler, C. Hoyt, R. Aggarwal and D. Calawa. This work is supported by the United States Air Force. Opinions, interpretations, conclusions and recommendations are those of the authors and are not necessarily endorsed by the United States Air Force.

REFERENCES

- ¹ T. Detleuphohn, K. Hiratazu, H. Amano and I. Akasaki, *Appl. Phys. Lett.* **61**, 2688 (1992).
- ² H.P. Maruska and J.J. Tietjen, *Appl. Phys. Lett.* **15**, 327 (1969).
- ³ W. Seifert, R. Franzheld, E. Butler, H. Sobotta and V. Riede, *Crysl. Res. Technol.* **18**, 383 (1983).
- ⁴ J. Neugebauer and C.G. Van de Walle, *Phys. Rev. B* **50**, 8067 (1994).
- ⁵ B. Baranov, L. Daweritz, V.B. Gutian, G. Jungk, H. Neumann and H. Raidt, *Phys. Status Solid. A* **49**, 629 (1978).
- ⁶ M. Illegems and H.C. Montgomery, *J. Phys. Chem. Solids* **34**, 885 (1973).
- ⁷ B.C. Chung and M. Gerstenson, *J. Appl. Phys.* **72**, 651 (1992).
- ⁸ T. Sasaki, *J. Cryst. Growth* **129**, 81 (1993).
- ⁹ K. Naniwa, S. Itoh, H. Amano, K. Itoh, K. Hiratazu and I. Akasaki, *J. Cryst. Growth* **99**, 381 (1990).
- ¹⁰ J.S. Hwang, A.V. Kuznetsov, S.S. Lee, H.S. Kim, J.G. Choi and P.J. Chong, *J. Cryst. Growth* **142**, 5 (1994).
- ¹¹ Work was performed at Charles Evans and Associates, West, Job # 47916.
- ¹² R. J. Mohar, R. Singh and T.D. Moustakas, *J. Electron. Mater.* **24**, 275 (1995).
- ¹³ R.J. Mohar and T.D. Moustakas, *J. Appl. Phys.* **76**, 4587 (1994).